Inorg. Chem. **2008**, *47*, 2864−2870

Unexpected C−H Activation of Ru(II)−Dithiomaltol Complexes upon Oxidation

Malin Backlund, Joseph Ziller, and Patrick J. Farmer*

Department of Chemistry, University of California, Irvine, California 92697-2025

Received November 7, 2007

Thione-substituted derivatives of maltol are of interest in several applications of metal-based drugs. In order to investigate the effect of the oxygenation on such thione chelates, Ru complexes of 3-hydroxy-2-methyl-4-thiopyrone (thiomaltol or Htma) and 3-hydroxy-2-methyl-4H-thiopyran-4-thione (dithiomaltol or Httma), $[Ru(bpy)_2(tma)]^+$, **1**, and $[Ru(bpy)_2(ttma)]^+$, **2**, were synthesized as diamagnetic PF_6^- salts. Peroxidation of **2** unexpectedly generated products of C−H activation at its pendant methyl group; an air-stable aldehyde $[Ru(bpy)_2(ttma\text{-}aldehyde)]^+$, **4**, was the major product. In addition, an intermediate oxidation product $[Ru(bpy)_2(ttma\text{-}alcohol)](PF_6)$, **3**, was characterized. Both **3** and **4** are also formed by reaction of **2** with outersphere oxidants (e.g., Na_2IrCl_6) and by bulk electrolysis under anaerobic conditions. Similar oxidations of the analogous $[Ru(bpy)_2(ettma)]^+$, **2′**, complex (3-hydroxy-2-ethyl-4H-thiopyran-4-thione; ethyl dithiomaltol or Hettma) formed the corresponding ketone, $[Ru(bpy)_2(ettma\text{-}ketone)](PF_6)$, **4′**, by oxidation at the same position adjacent to the conjugated ring. The structures of the aldehyde **4** and starting materials **1** and **2** have been confirmed by X-ray crystallography, and all complexes have been characterized by UV–vis, ^1H NMR, and IR spectroscopies. Initial mechanistic investigations are discussed.

Introduction

Sulfur oxygenation of thiones yields sulfine intermediates which are susceptible to S-atom extrusion, and the biological effect of thiones, such as dithiuram, has been proposed to be contingent on such *in vivo* sulfur extrusion.[1–6] We have shown that similar oxygenations of metal-bound thiones such as Ru(II) and Zn(II) dithiocarbamate complexes yield both S,S- and S,O-bound sulfine derivatives that can undergo both O- and S-atom extrusion.[7,8]

Scheme 1. Maltol and Related Ligands

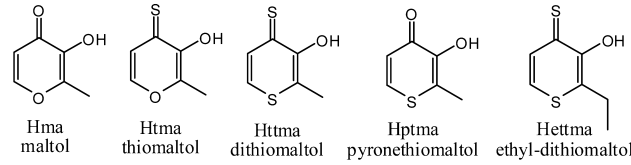

Metal−thione complexes derived from maltol are under current investigation for applications in metal transport, cancer therapy, and MMP inhibition, Scheme 1.[9–12] We hypothesized that these thione−metal chelates may also undergo S-based oxidation and extrusion. To test this hypothesis, the peroxygenation of thiomaltol and dithiomaltol was compared with and without complexation to an inert $[Ru(bpy)_2]^{2+}$ moiety, Schemes 2 and 3.

While peroxidations of the free ligands directly gave S-extruded products, similar reactions with Ru−dithiomaltol complexes yielded products of oxidation of the pendant

* Author to whom correspondence should be addressed. E-mail: pfarmer@uci.edu.

(1) Madan, A.; Faiman, M. D. *Drug Metab. Dispos.* **1994**, *22*, 324–330.
(2) Cen, D. Z.; Gonzalez, R. I.; Buckmeier, J. A.; Kahlon, R. S.; Tohidian, N. B.; Meyskens, F. L. *Mol. Cancer Ther.* **2002**, *1*, 197–204.
(3) Brar, S. S.; Grigg, C.; Wilson, K. S.; Holder, W. D.; Dreau, D.; Austin, C.; Foster, M.; Ghio, A. J.; Whorton, A. R.; Stowell, G. W.; Whittal, L. B.; Whittle, R. R.; White, D. P.; Kennedy, T. P. *Mol. Cancer Ther.* **2004**, *3*, 1049–1060.
(4) Cen, D. Z.; Brayton, D.; Shahandeh, B.; Meyskens, F. L.; Farmer, P. J. *J. Med. Chem.* **2004**, *47*, 6914–6920.
(5) Demaster, E. G.; Redfern, B.; Nagasawa, H. T. *Biochem. Pharmacol.* **1998**, *55*, 2007–2015.
(6) Hart, B. W.; Faiman, M. D. *Biochem. Pharmacol.* **1992**, *43*, 403–406.
(7) Brayton, D.; Tanabe, K.; Khiterer, M.; Kolahi, K.; Ziller, J.; Farmer, P. J. *Inorg. Chem.* **2006**, *45*, 6064–6072.
(8) Ng, S.; Ziller, J. W.; Farmer, J. P. *Inorg. Chem.* **2004**, *43*, 8301–8309.
(9) Puerta, D. T.; Lewis, S. A.; Cohen, S. M. *J. Am. Chem. Soc.* **2004**, *126*, 8388–8389.
(10) Puerta, D. T.; Cohen, S. M. *Inorg. Chem.* **2003**, *42*, 3423–3430.
(11) Monga, V.; Thompson, K. H.; Yuen, V. G.; Sharma, V.; Patrick, B. O.; McNeill, J. H.; Orvig, C. *Inorg. Chem.* **2005**, *44*, 2678–2688.
(12) Dikanov, S. A.; Liboiron, B. D.; Orvig, C. *J. Am. Chem. Soc.* **2002**, *124*, 2969–2978.

10.1021/ic7021962 CCC: $40.75
Published on Web 02/08/2008

Scheme 2

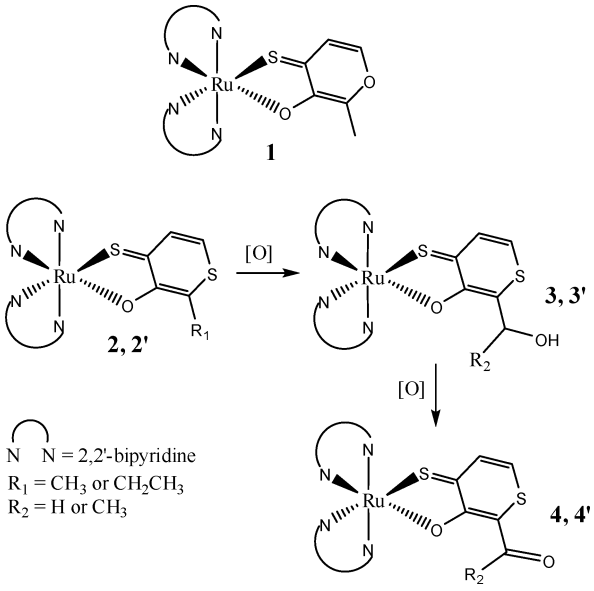

Scheme 3

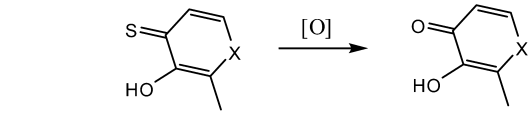

methyl or ethyl group. This report describes our investigations into this unusual activity.

Results and Discussion

The synthesis of the maltol-derived ligands (except hptma) in this study has been previously described.[13] The metal−thione complexes $[Ru(bpy)_2(tma)]^+$, **1**, $[Ru(bpy)_2(ttma)]^+$, **2**, and $[Ru(bpy)_2(ettma)]^+$, **2′**, were prepared by reaction of $Ru(bpy)_2Cl_2$ with the ligand at elevated temperatures. The resulting complexes were isolated as purple, diamagnetic PF_6^- salts. Further characterizations are given in the Supporting Information.

Identification of Oxidation Products. Reaction of free thiomaltol and dithiomaltol with an O-atom transfer agent such as urea hydrogen peroxide (UHP) induces S extrusion, in the latter case yielding a novel 3-hydroxy-2-methyl-4H-thiopyran (Hptma) in fair isolated yield, 31% by NMR analysis (Scheme 3). Treatment of **1** with O-atom transfer agents gave only ligand-decomposed products; electrospray ionization mass spectrometry (ESI-MS) and ^{1}H NMR analysis suggests these to be solvent-complexed $[Ru(bpy)_2]^{2+}$ species, implying that oxidation leads to ligand-decomposed species. Treatment of **2** and **2′** with the same agents yields the aldehyde and ketone derivatives, **4** and **4′**, respectively, as the major isolated products.

In a typical experiment, a 4-fold excess of oxone was added to a solution of **2** in CH_3CN at room temperature under an inert N_2 atmosphere and allowed to react overnight.

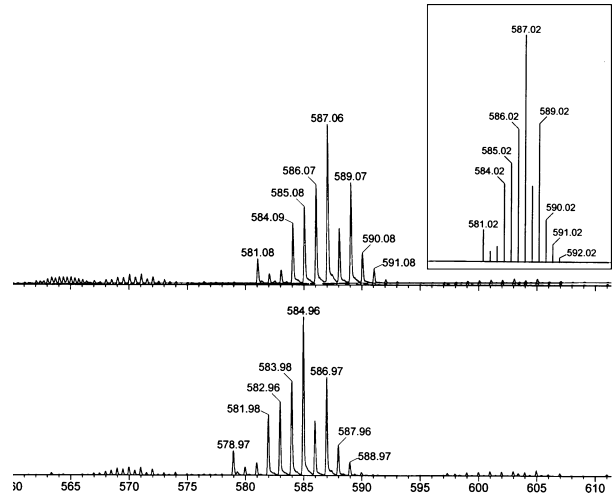

Figure 1. ESI-MS studies of the oxidation with oxone of $[Ru(bpy)_2(ttma-alcohol)]^+$, **3** (*m*/*z*: 587), to form $[Ru(bpy)_2(ttma-aldehyde)]^+$, **4** (*m*/*z*: 585). The top spectrum shows $[Ru(bpy)_2(ttma-alcohol)]^+$, and the bottom spectrum is the reaction after 5 h, showing a formation of complex **4**. Inserted in the box is the predicted isotopic envelope for complex **3**.

Column separation gave yields of ∼50% recovered **2**, 12% **3**, and 9% species **4**. Complex **4** was stable, characterized as an aldehyde by ^{1}H NMR, and its structure subsequently confirmed by X-ray crystallography.

Complex **3** is air-sensitive and prone to decomposition but has been characterized by ESI-MS, ^{1}H NMR, and FT-IR. The mass spectrum of **3** showed a characteristic [**2** + 16] *m*/*z* parent ion, indicative of the addition of a single oxygen atom. First, it was expected that the intermediate, **3**, was oxygenated at the ring sulfide, for example, a sulfoxide, which might then convert to the observed C-oxygenated product via subsequent rearrangement. Therefore, 2D correlation spectroscopy (COSY) NMR spectra of **2** and **3** were obtained for structural comparisons (Supporting Information, Figures S2 and S3), and the only substantive difference is a shift of ca. 0.10 ppm of the proton α to the sulfide. In addition, the NMR spectrum of **3** does not display splitting indicative of the expected chirality for a sulfoxide (Supporting Information, Figure S7). However, most persuasive was the FT-IR spectrum of **3**, which showed a new peak at 1125 cm^{-1}, more reasonably assigned to a C−O stretch rather than to a S−O stretch.[14]

To gain further insight into the identity of **3**, several reactivity studies were carried out. The reaction of **3** with oxygenating agents (oxone, UHP) forms the aldehyde **4**, Figure 1. Treatment of **3** with typical alkylating agents, acetyl chloride and MeI, yields stable products, as characterized by ESI-MS (Scheme 4). This is consistent with the expected reactivity of an alcohol, but not that of a sulfoxide, Supporting Information, Figure S4.

Oxidizing Agents. Initially, a series of peroxidation reagents, such as oxone, *m*-chloroperbenzoic acid (mCPBA), and UHP, was found to give similar yields of ca. 15% of **3** and **4** after the reaction of excess reagent with **2** (data not shown). Other reagents, such as 2,6-dicarboxypyridinium

(13) Brayton, D. F.; Jacobsen, F. E.; Cohen, S. M.; Farmer, P. J. *J. Chem. Soc., Chem. Commun.* **2006**, 206–208.

(14) Pavia, D. L.; Lampman, G. M.; Kriz, G. S. *Introduction to Spectroscopy*; Thompson Learning Inc.: Philadelphia, 2001.

Scheme 4

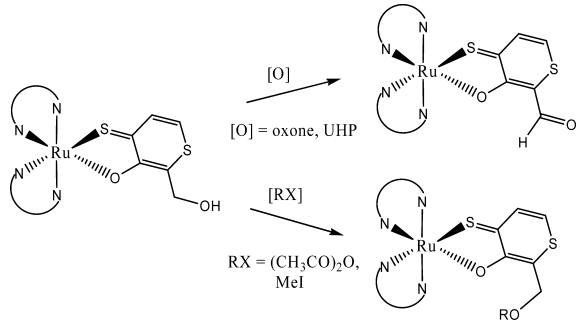

Table 1. Comparative Yields of **4** Obtained by Oxidation of **2** with Various Reagents

reagent	solvent	reaction time	equiv. per Ru	yield[a]
UHP	MeCN	24 h	2 equiv	2%
		48 h		5%
oxone	MeCN	24 h	2 equiv	4%
		48 h		6%
IBX	MeCN	24 h	3 equiv	28%
		48 h		30%
Na_2IrCl_6	MeCN w/H_2O	24 h	4 equiv	5%
		48 h		10%
Na_2IrCl_6	MeCN w/NaOH	1 h	4 equiv	10%

[a] Comparative percentage yields were determined by ESI-MS using $[Ru(bpy)_2(m\text{-}DTC)]^+$ (complex **1** in ref 8) as an added internal standard after the reaction was quenched.

chlorochromate (2,6-DCPCC), were also found to yield similar product yields; however, much larger yields of complex **4** were obtained from reactions with 2-iodoxybenzoic acid (IBX) and $Na_2Ir(IV)Cl_6$. Similarly, complex **3** was obtained under anaerobic conditions, suggesting that the O atom is obtained from adventitious water.

A comparative quantification of this reactivity was determined by using stoichiometric oxidations of **2** with selected reagents, Table 1. In a typical reaction, a stoichiometric amount of UHP (0.003 g, 0.035 mmol) was added to an aerobic solution of **2** (0.013 g, 0.018 mmol) in CH_3CN. After ~24 h, a sample was removed for ESI-MS studies, and a peak was observed at *m*/*z* 585 corresponding to complex **4**. Reported yields in Table 1 are for comparison, as determined against an added standard, and are less than isolated yields obtained in larger-scale reactions. For example, ^1H NMR quantification after chromatography gave a yield of 41% of **4** from the reaction of **2** with 3 equiv of IBX, and only 28% by ESI-MS, as reported in Table 1. Monitoring the reaction by UV–vis under the same conditions, Figure 2, shows an apparent clean conversion from **2** to **4** over 3 h; no buildup of intermediate species is seen.

In addition, oxidations of **2** with $Na_2Ir(IV)Cl_6$ in dry $MeOH/NaOCH_3$ resulted in products observed by ESI-MS consistent with the addition of one and two methoxy groups to complex **2**, [**2** + 30] and [**2**+ 60] *m*/*z* in Figure 3, analogous to the addition of sequential water molecules resulting in complexes **3** and **4**. The formation of these methoxy adducts suggests that the C−H activation occurs through a cationic intermediate susceptible to solvent attack.

Electrochemical Studies. Cyclic voltammograms of complexes **1**–**4** in CH_3CN are shown in Figure 4, and derived

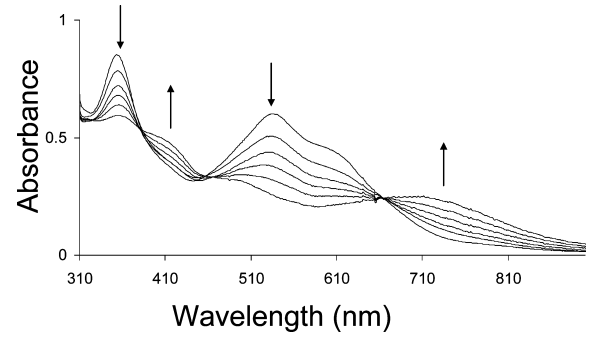

Figure 2. Sequential electronic absorbance spectra of the reaction of complex **2** with 3 equiv of IBX in CH_3CN at room temperature. The reaction was monitored for 150 min, and a spectrum was taken every 30 min. The final spectrum is similar to that of the aldehyde, **4**.

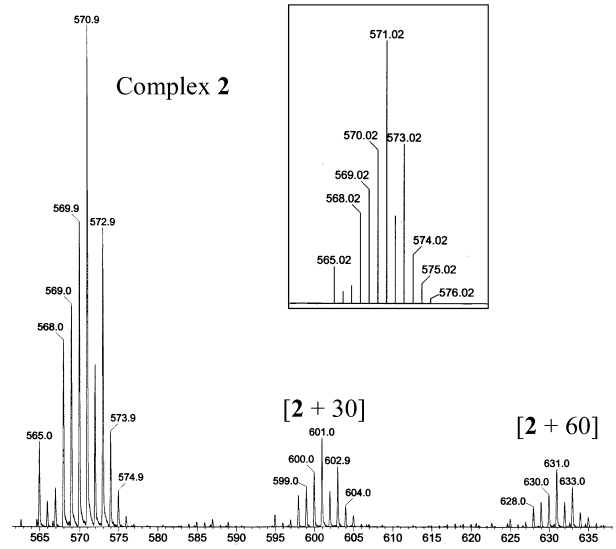

Figure 3. ESI-MS studies of the reaction of $[Ru(bpy)_2(ttma)]^+$, **2**, with Na_2IrCl_6 in dry MeOH/NaOMe to form apparent methoxy adducts at *m*/*z* 601 and 631. Inserted in the box is the predicted isotopic envelope for complex **2**.

parameters are given in Table 2. Electrochemically reversible oxidation couples are observed for complexes **1**, **2**, and **4**, with ΔE_p equal to ca. 65 mV and i_{pa}/i_{pc} close to unity. In contrast, the oxidation of complex **3** appears quasi-reversible, with the i_{pa}/i_{pc} ratio decreasing from unity at slower scan rates, signifying a loss of the oxidized species by a following chemical reaction. Also, a small oxidation wave is seen at ca. 800 mV, close to that of **4**, from an apparent product of the initial oxidation. The similarity of the oxidation potentials of complexes **1** and **2**, with the different tma and ttma ligands, suggests that the initial oxidation is metal-based. The positive shift in potential for complex **4** is consistent with the addition of an electron-withdrawing group on the ligand and likewise suggests that it would be more stable to oxidizing or oxygenating reagents.

Analysis of the voltammograms predicts the dominance of **4** as the bulk oxidation product of **2**. The intermediate product, **3**, is oxidized at a potential close to the starting complex, **2**, and thus cannot accumulate during bulk oxidations. After repeated scans, voltammograms of **3** obtained broad and overlapping oxidation waves, confirming the existence of mixtures of oxidized products being generated.

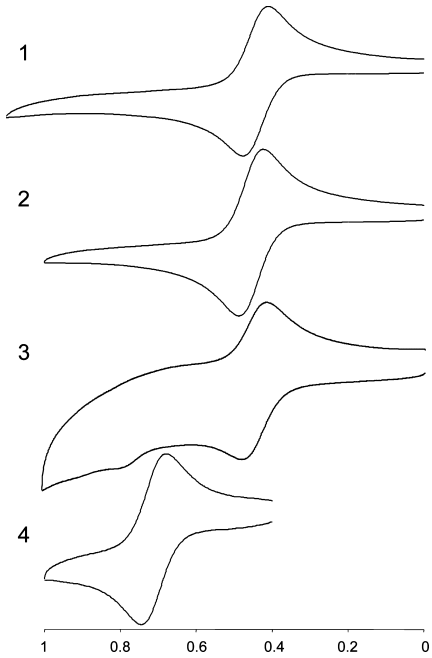

Figure 4. Cyclic voltammograms of complexes **1**–**4**, conditions: 0.1 M $TBAPF_6$ in anaerobic MeCN, Pt working and counter electrodes, reference Ag/AgCl.

Table 2. Electrochemical Data for Complexes **1**–**4**[a]

complex	$E_{1/2}$ (mV)	ΔE_p (mV)	i_{pa}/i_{pc}
1 $[Ru(bpy)_2(tma)]^+$	+445	65	0.96
2 $[Ru(bpy)_2(ttma)]^+$	+455	62	0.97
3 $[Ru(bpy)_2(ttma\text{-alcohol})]^+$	+446	64	0.78
4 $[Ru(bpy)_2(ttma\text{-aldehyde})]^+$	+713	65	0.90

[a] All potentials measured using Ag/AgCl reference electrode, Pt disc working electrode, and Pt wire counter electrode; scan rate of 100 mV/sec in MeCN, 0.1 M $TBAPF_6$.

Table 3. Structural Data and Comparison of Complexes **1**, **2**, and **4**

	complex **1**	complex **2**	complex **4**
cryst syst	monoclinic	monoclinic	triclinic
space group	$P2_1/n$	$C2/c$	$P1$
color	purple	purple	black
Ru−O (Å)	2.080(15)	2.107(6)	2.086(2)
Ru−S (Å)	2.362(6)	2.320(2)	2.315(9)
ΔC−C (Å)	0.098	0.108	0.108
N−Ru−O (deg)	172.9(7)	172.9(2)	174.4(10)
N−Ru−S (deg)	170.3(5)	172.0(19)	171.1(8)

Bulk electrolysis of **2** at 600 mV (normal hydrogen electrode) was carried out using large-area gold plate working and counter electrodes. After ∼12 h, the electrolysis mixture was analyzed by cyclic voltammetry, Figure 5, which demonstrated the formation of the aldehyde. Square-wave voltammetric analysis of the resulting solution gave the yield of **4** as ca. 40%.

Electron Paramagnetic Resonance (EPR) Characterization of Initial Product of Oxidation. As the species **3** and **4** are generated by sequential two-electron oxidations of complex **2**, efforts were made to characterize possible one-electron oxidized species involved. In addition, complex **2** was reacted with 1 equiv of $Ir(IV)Cl_6$ in a dry box; EPR analysis of the reaction mixture after 1 h at 77 K shows a broad structured peak (>1000 G) with a g_{avg} value of 1.95, well below that expected for a free organic radical (Supporting Information, Figure S6). This signal is attributable

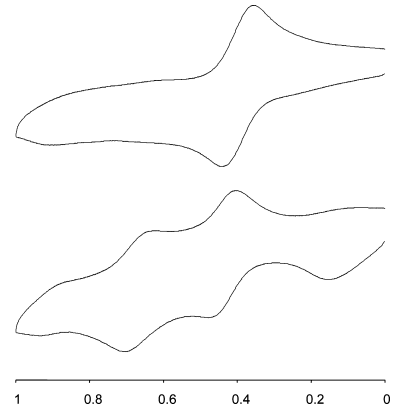

Figure 5. Cyclic voltammograms before (top) and after (bottom) anaerobic electrolysis of complex **2** at +650 mV for 12 h. Conditions: 0.1 M $TBAPF_6$ in anaerobic MeCN, Pt working and counter electrodes, reference Ag/AgCl.

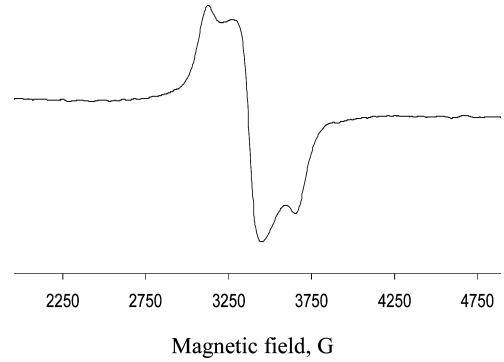

Figure 6. X-band EPR spectrum at 10 K of CH_3CN solution of **2** after reaction with 1 equiv of Na_2IrCl_6. Conditions: microwave frequency, 9.64 GHz; microwave power, 2.02 mW; modulation amplitude, 4.00 G; time constant, 164 ms; sweep width, 3300 G; sweep time, 21.0 ms.

to the initial oxidization product of **2**, and is consistent with a Ru(III) d^5 S = ½ system of pseudo-C_{2v} symmetry with significant broadening due to spin–orbit coupling. Within the broad absorbance, small rhombic features are observable but difficult to assign. Cooling the same sample to 10 K allowed resolution of these features, Figure 6, as an anisotropic absorbance peaks with g values of 2.204, 2.046, and 1.886. Similar rhombic signals have been observed for a $Ru(III)(L^1)$-$(L^2)_2$ species in pseudo-C_{2v} coordination environments.[15,16]

A sample of the bulk electrolysis solution after voltammetric analysis in Figure 5 was also analyzed by EPR at 77 K; the resulting spectrum again showed a broad low-intensity signal with a $g_{avg} = 1.99$, with small anisotropic features at $g = 2.10$ and 1.93 (Supporting Information, Figure S6). Assignment of this spectrum is difficult as the solution contains a mixture of species, but the rhombic splitting is distinct from that of oxidized **2** and still readily attributed to a metal-based rather than organic radical.

Structural Characterizations. Salts of the cationic complexes **1**, **2**, and **4** have been characterized by X-ray diffraction studies (Supporting Information, Figure S5). Slow vapor diffusion of diethyl ether into CH_2Cl_2 solutions of

(15) Lever, A. B. P.; Auburn, P. R.; Dodsworth, E. S.; Haga, M. A.; Liu, W.; Melnik, W.; Nevin, A. *J. Am Chem Soc.* **1988**, *110*, 8076–8084.
(16) Haga, M. A.; Dodsworth, E. S.; Lever, A. B. P. *Inorg. Chem.* **1986**, *25*, 447–453.

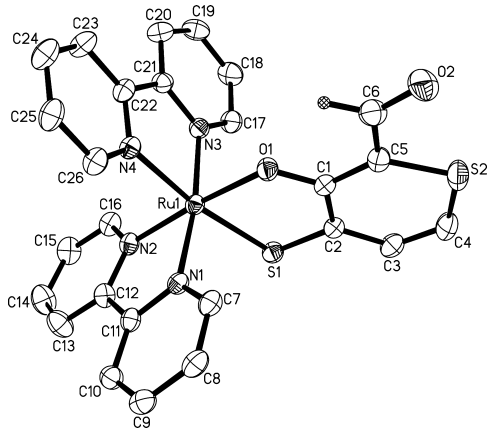

Figure 7. Crystal structure of $[Ru(bpy)_2(ttma\text{-}aldehyde)]^+$, **4**.

Scheme 5

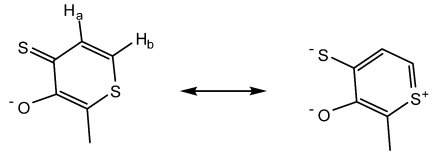

Thiopyrilium

cationic complexes **1**, **2**, and **4** as PF_6 salts yielded crystals suitable for X-ray diffraction studies. Purple crystals of complexes **1** and **2** are monoclinic, and in space groups $P2_1/n$ and C_2/c, respectively, while the black crystals of complex **4** are triclinic in the P_1 space group, Table 3.

The X-ray diffraction analysis of **4**, Figure 7, confirms its characterization as an aldehyde; the observed C(6)−O(2) bond length is 1.225 Å, which is appropriate for a carbon−oxygen double bond.[17] The Ru coordination sphere in all three structures is only slightly distorted from octahedral, due to constrained bite angles of the maltol-derived ligands. The Ru−S bond length decreases from complex **1** to **2**, while that of the Ru−O bond lengthens, perhaps indicative of tighter Ru−S interactions in the latter complex. Variations in the maltol-ligand C−C bond lengths were analyzed for the three complexes, as a measure of delocalization within the complexed ligand. The observed differences of ca. 0.1 Å indicate significant bond delocalization, as ΔC−C values for nonaromatic systems are >0.2 Å.[18]

Mechanistic Considerations. The C−H oxidations of complex **2** resemble the comparable oxidations of benzylic carbons and, by analogy, suggest some aromaticity to the ttma ring. There is much precedence for aromaticity of the related thiopyriliums, an oxidized form of the ttma ring shown in Scheme 5.[19,20] Crystallographic data of **2** do provide evidence of delocalization within the ttma ring. Delocalization in **1** and **2** can be assessed by NMR, as measured by the effect of ring current on proton signals (H_a and H_b in Scheme 5). The magnitude of ring current in a system is measured from the average chemical shift, $(\delta_a + \delta_b)/2$, which is δ 7.74 for **2** compared to δ 7.44 for **1**.[21] This suggests that complex **2** has a greater ring current and thus more delocalization than **1**.

Scheme 6

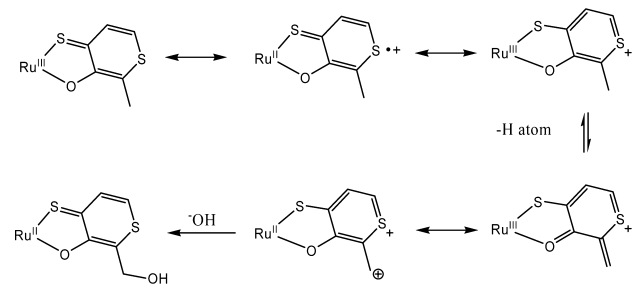

Delocalization in the ttma ligand is likely increased in the singly oxidized state, as the thiopyrilium resonance structure would be favored to neutralize the greater charge on a Ru(III) center. EPR characterization of the initial oxidation product yielded an anisotropic spectrum at low temperatures, implying that the unpaired electron has significant metal-based character.[22–25] Thus, it may be the nature of the singly oxidized intermediate that induces the C−H activation in the ttma complex, **2**, and not the tma complex, **1**.

In this system, C-oxidized products are obtained by reaction of **2** with O-atom transfer agents (oxone, mCPBA, and UHP) and chemical oxidants (Na_2IrCl_6 and IBX) and by electrochemical oxidation. The formation of C-oxidized products from complex **2** by reaction with Na_2IrCl_6 or by bulk electrolysis is consistent with an outersphere single-electron transfer as the initiating event.

The highest yields of C−H activated products are obtained in reactions using IBX, a periodinane reagent previously shown to oxidize carbons adjacent to conjugated systems, giving aldehyde and ketone products, with regioselectivity influenced by the conjugation.[26–29] IBX is a multifaceted reagent in that it may act as an electron acceptor, a H-atom abstractor, and an O-atom donor, all of which may be involved in its reactivity with **2**.

Scheme 6 illustrates one possible mechanism for the initial transformation of **2** to **3**, starting from the singly oxidized product of $\mathbf{2}^+$. Delocalization of the unpaired electron over both the Ru and the ttma ligand is possible, but we suggest

(17) Dewar, M. J. S.; Thiel, W. *J. Am. Chem. Soc.* **1977**, *99*, 4907–4917.
(18) Von Ragué Schleyer, P.; Jiao, H. *Pure Appl. Chem.* **1996**, *68*, 209–218.
(19) Smithermann, H. C.; Ferguson, L. N. *Tetrahedron* **1968**, *24*, 923–932.
(20) Saieswari, A.; Priyakumar, D.; Sastry, N. *THEOCHEM* **2003**, *663*, 145–148.
(21) Jonas, J.; Derbyshire, W.; Gutowsky, H. S. *J. Phys. Chem.* **1965**, *69*, 1–5.
(22) Dhara, P. K.; Drew, M. G. B.; Chattopadhyay, P. *Polyhedron* **2006**, *25*, 1939–1945.
(23) Lahiri, G. K.; Bhattacharya, S.; Ghosh, B. K.; Chakravorty, A. *Inorg. Chem.* **1987**, *26*, 4324–4331.
(24) Dos Santos Silvia, H. A.; McGarvey, B. R.; de Almeida Santos, R. H.; Bertotti, M.; Mori, V.; Franco, D. W. *Can. J. Chem.* **2001**, *79*, 679–687.
(25) Kuan, S. L.; Leong, W. K.; Goh, L. Y. *Organometallics* **2005**, *24*, 4639–4648.
(26) Nicolaou, K. C.; Baran, P. S.; Zhong, Y. L. *J. Am. Chem. Soc.* **2001**, *123*, 3183–3185.
(27) Nicolaou, K. C.; Montagon, T.; Baran, S.; Zhong, Y. L. *J. Am. Chem. Soc.* **2002**, *124*, 2245–2258.
(28) Nicolaou, K. C.; Mathison, C. J. N.; Montagnon, T. *J. Am. Chem. Soc.* **2004**, *126*, 5192–5201.
(29) Shibuya, M.; Ito, S.; Takahashi, M.; Iwabuchi, Y. *Org. Lett.* **2004**, *6*, 4303–4306.

that aromaticity in the thiopyrylium cation enables the activation of the pendant methyl group. The formation of the alcoholic product requires a second proton-coupled oxidation, and the facility of IBX in this reaction suggests that this may take the form of a H-atom abstraction. Extensive delocalization allows formation of a carbocationic intermediate that would likely precede the addition of solvent (water or methanol) at the oxidized carbon. An analogous pathway would yield the aldehyde upon oxidation of the alcoholic intermediate.

An alternative is to invoke sequential deprotonations and oxidations. Potentiometric titrations of complex **2** in dry MeOH from pH 11.5 to 1.5 gave no indication of protonation or deprotonation within this range. Oxidations run under basic conditions, for example, with 4 equiv of NaOH in MeCN, Table 1, showed only small increases in product formation. Likewise, reactions with added NaOMe in MeOH showed relatively modest increases in yield of methoxy adducts. Thus, we surmise a rate-limiting step may be radical-dependent.

Conclusions

The α-hydroxyl thione Ru complexes **2** and **2′** undergo unexpected C−H activation of the methyl and methylene groups to form aldehyde and ketone products. The ability of various O-atom transfer agents, outersphere oxidants, and bulk electrochemical oxidations to form these products implies that the initiating step is electron transfer; we propose that C−H activation proceeds due to thiopyrylium-like aromaticity of the initially oxidized form.

The observed C oxidations are unusual in that the two S sites on the ttma ligand were unaffected. Similar reactions of the ligands alone yield the expected S-extruded products; therefore, the coordination of the ligand to the $[Ru(bpy)_2]^{2+}$ center is crucial for the C−H activation to take place. However, the question to why C−H activation is more favorable than S-oxidation in this case remains elusive.

Experimental Section

Abbreviations. *cis*-Dichloro-bis-2,2-bipyridineruthenium(II) ($Ru(bpy)_2Cl_2$), dithiomaltol (Httma), ethyl-dithiomaltol (Hettma), dithiomaltol-aldehyde (Httma-aldehyde), ethyl-dithiomaltol-ketone (Hettma-ketone), pyronethiomaltol (Hptma), potassium peroxomonosulfate (oxone), *m*-chloroperbenzoic acid (mCPBA), 2,6-dicarboxypyridinium chlorochromate (2,6-DCPCC), urea hydrogen peroxide (UHP), and 2-iodoxybenzoic acid (IBX).

Materials. *cis*-Dichlorobis(2,2′-bipyridine) ruthenium(II) dihydrate, 99%, was purchased from Strem Chemicals. Basic alumina was purchased from Fisher Scientific, and all other chemicals were purchased from Aldrich Chemical Co. Httma and Hettma were synthesized following published procedures.[13] The oxidant 2,6-DCPCC was generated in situ following a published procedure, by reacting CrO_3 with pyridinium 2,6-dicarboxylic acid in 6 M HCl for 2 h.[30] All common laboratory solvents are of reagent grade and were dried and degassed using standard techniques. Manipulations requiring anaerobic conditions were carried out under nitrogen on a Schlenk line or in a glovebox. All reactions involving complexes containing the $[Ru(bpy)_2]^{2+}$ moiety were carried out in the dark.

Physical Measurements. Mass spectra were determined using a Micromass LCT machine. UV−vis spectra were recorded using a Perkin-Elmer Lambda 900 machine. ^{1}H NMR spectra were recorded on Bruker Avance 400 and 500 MHz spectrometers. Chemical shifts were referenced via the solvent signal. X-band EPR spectra were recorded on a Burker spectrometer. Experiments were carried out at liquid nitrogen temperature (77 K) and liquid helium temperature (10 K). Infrared spectra were recorded on an Impact 410 machine from Nicolet as KBr pellets. Elemental analyses were performed by Atlantic Microlab, Norcross, GA. All single-crystal X-ray diffraction structures were solved by the X-ray Crystallography Facility at UCI.

Synthesis of $[Ru(bpy)_2(tma)](PF_6)$, 1. $Ru(bpy)_2Cl_2$ (0.454 g, 0.937 mmol) and Htma (0.266 g, 1.90 mmol) were placed in a three-neck flask with 5 mL of ethylene glycol. The three-neck flask was fitted with a condenser, and an inert atmosphere was established using standard Schlenk techniques. The reaction was brought to 130 °C and stirred under N_2 for 45 min. The mixture was then poured into 200 mL of deionized H_2O, and an excess of KPF_6 was added. The purple product was collected on a Buchner funnel under vacuum filtration. The compound was purified using a basic alumina column and CH_2Cl_2/CH_3CN as the eluent. The isolated yield was 0.462 g (89%). The compound was crystallized in CH_2Cl_2/ diethyl ether, forming purple needle-shaped crystals suitable for X-ray diffraction. ESI MS: *m*/*z* 555. ^{1}H NMR (500 MHz, CD_3OD): δ 9.52 (d, 1H), 8.73 (d, 1H), 8.63 (d, 1H), 8.58 (d, 2H), 8.44 (d, 1H), 8.09 (t, 2H), 7.96 (t, 1H), 7.86 (d, 1H), 7.80 (t, 1H), 7.74 (d, 1H), 7.71 (d, 1H), 7.67 (t, 1H), 7.61 (t, 1H), 7.40 (d, 1H), 7.32 (t, 1H), 7.15 (t, 1H), 2.27 (s, 3H). Anal. calc for $RuN_4C_{26}O_2SH_{21}PF_6 \cdot CH_2Cl_2$: C, 41.28; H, 3.08; N, 7.13. Found: C, 40.75; H, 3.08; N, 7.55.

Synthesis of $[Ru(bpy)_2(ttma)](PF_6)$, 2. $[Ru(bpy)_2(ttma)](PF_6)$ was synthesized by the same procedure used for **1**, starting from $Ru(bpy)_2Cl_2$ (0.350 g, 0.723 mmol) and Httma (0.228 g, 1.45 mmol). The product was obtained as a purple solid. The isolated yield was 0.295 g (72%). The compound was crystallized in CH_2Cl_2/ EtO_2, forming purple crystals suitable for X-ray diffraction. ESI MS: *m*/*z* 571. ^{1}H NMR (500 MHz, CD_3OD): δ 9.54 (d, 1H), 8.65 (d, 1H), 8.61 (d, 1H), 8.58 (d, 2H), 8.45 (d, 1H), 8.08 (t, 2H), 8.05 (d, 1H), 7.97 (t, 1H), 7.90 (d, 1H), 7.79 (t, 1H), 7.71 (d, 1H), 7.64 (t, 1H), 7.64 (d, 1H), 7.58 (t, 1H), 7.32 (t, 1H), 7.15 (t, 1H), 2.06 (s, 3H). Anal. calc for $RuN_4C_{26}OS_2H_{21}PF_6$: C, 43.64; H, 2.96; N, 7.83. Found: C, 44.32; H, 3.19; N, 7.73.

Oxidation of Httma, Isolation of Hptma. Httma (0.15 g, 0.945 mmol) was dissolved in 20 mL of CH_3CN and placed in a round-bottom flask fitted with a N_2 inlet adaptor. UHP (0.36 g, 3.80 mmol) was dissolved in 10 mL of CH_3OH and added to the round-bottom flask. The reaction was stirred under N_2 for ∼24 h. The dark green reaction mixture was then dried *in vacuo* and dissolved in $CHCl_3$ followed by an aqueous wash (4 × 100 mL). The $CHCl_3$ layer was dried over $MgSO_4$ for ∼3 h, followed by evaporation of the solvent *in vacuo*, giving a brown solid. Isolated yield for Hptma: 0.024 g (16%). ESI MS: *m*/*z* 143 [M]+H. ^{1}H NMR (500 MHz, $CDCl_3$): δ 7.74 (d, 1H), 7.17 (d, 1H), 2.41 (s, 3H). Anal. calc for $C_6H_5O_2S \cdot CH_3OH$: C, 48.26; H, 5.79. Found: C, 48.52; H, 6.18.

Oxidation of 1. $Ru(bpy)_2(tma)$ (0.010 g, 0.018 mmol) and 2,6-DCPCC (0.010 g, 0.034 mmol) were dissolved in CH_3CN and added to a 50 mL round-bottom flask inside a N_2 purged dry box. The reaction was monitored by ESI-MS, and after ∼20 min, a ligand decomposed peak at *m*/*z* 441 ([M]−114) was observed (Supplorting

(30) Tajbakhsh, M.; Hosseinzadeh, R.; Niaki, M. Y. *J. Chem. Res.* **2002**, *10*, 508–510.

Information, Figure S1). Similar results were observed for the reaction of **1** with other oxidants.

Oxidation of 2; isolation of [Ru(bpy)$_2$(ttma-alcohol)](PF$_6$), 3, and [Ru(bpy)$_2$(ttma-aldehyde), 4. Ru(bpy)$_2$(ttma) (0.080 g, 0.112 mmol) and 2,6-DCPCC (0.200 g 0.667 mmol) were dissolved in CH_3CN and added to a 100 mL round-bottom flask fitted with a nitrogen inlet adaptor. The reaction was carried out in an inert N_2 atmosphere under stirring for 24 h. The solvent was removed in vacuo, and the products were isolated using an alumina basic column with $CH_2Cl_2/CH_3CN/CH_3OH$ as the eluents. Complexes **3** and **4** were obtained as separate bands off the alumina column. Further purification was made using a second column with the same stationary phase and eluent. The isolated yields were 0.010 g (12%) of **3** and 0.0075 g (9.2%) of **4**.

Compound **4** was crystallized in CH_2Cl_2/EtO_2, forming black single crystals suitable for X-ray diffraction. ESI MS: *m/z* 585. UV/vis (nm): 380, 497, 718. ^{1}H NMR (400 MHz, CD_3OD): δ 9.96 (s, 1H), 9.22 (d, 1H), 8.61 (m, 4H), 8.49 (d, 1H), 8.14 (d, 1H), 8.12 (d, 1H), 8.12 (d, 1H), 8.02 (t, 1H), 7.92 (d, 1H), 7.87 (d, 1H), 7.86 (t, 1H), 7.71 (t, 1H), 7.64 (m, 2H), 7.38 (t, 1H), 7.21 (t, 1H). Anal. calc for $RuN_4C_{26}O_2S_2H_{19}PF_6 \cdot C_5H_{12}$: C, 46.44; H, 3.90; N, 6.99. Found: C, 46.39; H, 3.44; N, 6.81.

Attempts to crystallize **3** were made using slow vapor diffusion in CH_2Cl_2/Et_2O, but no single crystal could be isolated. Likewise, elemental analysis was problematic. ES/MS: *m/z* 587. UV/vis (nm): 355, 532. FT-IR (cm^{-1}): ν(C=C) 850, ν(C−O) 1100. ^{1}H NMR (400 MHz, CD_3CN): δ 9.44 (d, 1H), 8.58 (d, 1H), 8.40 (m, 3H), 8.28 (d, 1H), 8.00 (m, 3H), 7.90 (m, 2H), 7.72 (t, 1H), 7.64 (m, 2H), 7.53 (m, 2H), 7.24 (t, 1H), 7.07 (t, 1H).

Synthesis of [Ru(bpy)$_2$(ettma)](PF$_6$), 2′. Samples of [Ru(bpy)$_2$(ettma)](PF$_6$) were synthesized by the same procedure used for **1**, starting from Ru(bpy)$_2$Cl$_2$ (0.625 g, 1.29 mmol) and Hettma (0.220 g, 1.29 mmol). The product was obtained as a purple solid. The isolated yield was 0.590 g (63%). ESI MS: *m/z* 585. UV/vis (nm): 357, 539. ^{1}H NMR (500 MHz, CD_3OD): δ 9.48 (d, 1H), 8.61 (d, 1H), 8.54 (d, 1H), 8.52 (d, 2H), 8.42 (d, 1H), 8.01 (m, 3H), 7.94 (d, 1H), 7.91 (d, 1H), 7.75 (t, 1H), 7.65 (d, 1H), 7.59 (m, 2H), 7.52 (t, 1H), 7.28 (t, 1H), 7.11 (t, 1H), 2.62 (q, 1H), 2.47 (q, 1H), 0.87 (t, 3H). Anal. calc for $RuN_4C_{27}OS_2H_{23}PF_6$: C, 44.44; H, 3.18; N, 7.68. Found: C, 44.37; H, 3.14; N, 7.52.

Oxidation of 2′; Isolation of [Ru(bpy)$_2$(ettma-alcohol)](PF$_6$), 3′, and [Ru(bpy)$_2$(ettma-ketone)](PF$_6$), 4′. [Ru(bpy)$_2$(ettma-alcohol)](PF$_6$) was synthesized using the same procedure used for **2**, starting with [Ru(bpy)$_2$(ettma)]$^+$ (0.200 g, 0.274 mmol) and 2,6-DCPCC (0.164 g, 0.548 mmol). The complexes were separated on an alumina basic column. Complex **3′** was isolated as a purple salt (7.8% yield). ESI MS: *m/z* 601. UV/vis (nm): 357, 538. ^{1}H NMR (500 MHz, CD_3OD): δ 9.47 (d, 1H), 8.60 (m, 4H), 8.44 (d, 1H), 8.03 (m, 4H), 7.95 (t, 1H), 7.77 (m 2H), 7.62 (m, 2H), 7.53 (t, 1H), 7.30 (t, 1H), 7.14 (t, 1H), 1.35 (q, 2H), 0.83 (t, 3H). Complex **4′** was isolated as a purple salt, and the isolated yield was 0.011 g (4%). ESI MS: *m/z* 599. UV/vis (nm): 374, 510, 684. ^{1}H NMR (500 MHz, CD_3OD): δ 9.28 (d, 1H), 8.62 (d, 2H), 8.60 (d, 1H), 8.55 (d, 1H), 8.50 (d, 1H), 8.13 (m, 2H), 8.08 (d, 1H), 8.02 (m, 2H), 7.87 (d, 1H), 7.85 (d, 1H), 7.69 (m, 2H), 7.62 (t, 1H), 7.37 (t, 1H), 7.22 (t, 1H), 1.98 (s, 3H). FT-IR (cm^{-1}): 1622 (C=O). Anal. calc for $RuN_4C_{27}O_2S_2H_{21}PF_6 \cdot H_2O$: C, 42.58; H, 3.04; N, 7.36. Found: C, 42.80; H, 3.05; N, 7.16.

Oxidation of 2 with IBX. Ru(bpy)$_2$(ttma) (0.01 g, 0.011 mmol) and IBX (0.01 g 0.042 mmol) were dissolved in CD_3CN and added to a 50 mL round-bottom flask fitted with a nitrogen inlet adaptor. The reaction was carried out in an inert N_2 atmosphere under stirring and was monitored by ^{1}H NMR and ESI-MS. After 2 h, the aldehyde peak was observed by NMR (∼10 ppm) and ESI-MS (*m/z* 585). A quantitative yield determination from the reaction of Ru(bpy)$_2$(ttma-aldehyde; 0.010 g, 0.014 mmol) with IBX (0.026 g, 0.093 mmol; 3 equiv of IBX) in 10 mL CH_3CN was carried out. The mixture was purified on basic alumina with CH_3CN/MeOH as eluents. The yield of complex **4** was determined as 41% by ^{1}H NMR.

UV/Visible Studies of Oxidation of Complex 2. Standard solutions of Ru(bpy)$_2$(ttma) (0.084 mM) and IBX (1.12 mM) in CH_3CN were prepared separately in a 50 mL volumetric flask and a 100 mL volumetric flask, respectively. Complex **2** (2 mL) was placed in a capped UV/vis cell followed by the addition of IBX (3 equiv, 1 mL). The reaction was monitored every 30 min for 150 min. The spectrum shows a direct conversion from the starting material to the aldehyde, **4**.

Oxidation of 2 with Ir(IV). Ru(bpy)$_2$(ttma) (0.005 g, 0.007 mmol) was treated with sodium hexachloridoiridate(IV) (0.006 g, 0.014 mmol) in CH_3CN with ca. 2% water by volume. The reaction was left overnight, and ESI-MS (*m/z*: 585) and ^{1}H NMR confirmed the formation of the aldehyde. In a separate experiment, complex **2** was reacted with 4 equiv of Na_2IrCl_6 (18 umol **2**, 70 umol Na_2IrCl_6) in 5 mL of CH_3CN and ca. 4 equiv of NaOH (0.5 mL 0.1 M NaOH). A similar experiment was run in methanol with 10-fold excess NaOMe (7 umol **2**, 28 umol Na_2IrCl_6, 4 mg NaOMe, in 2 mL of CH_3CN); after 1 h, ESI-MS showed the formation of the ether complex, in 12% yield, and 10% diether, Figure 3. When 4 equiv of Na_aIrCl_6 was used, the observed yields increased to 20% and 15%, respectively.

Reaction of 3 and 3′ with Oxidants. Oxidation of [Ru(bpy)$_2$(ttma-alcohol)](PF$_6$) was carried out in a 25 mL round-bottom flask using a 4-fold excess of oxone as the O-atom transfer agent. The reaction was carried out on the NMR scale with CD_3CN as the solvent and was followed by ^{1}H NMR and ESI-MS. Formation of [Ru(bpy)$_2$(ttma-aldehyde)](PF$_6$), **4**, was seen after 1 h. The reaction was monitored for 24 h, and complete formation of **4** was observed. [Ru(bpy)$_2$(ttma-alcohol)](PF$_6$), **3′**, was reacted with oxone as well, and formation of [Ru(bpy)$_2$(ettma-ketone)]$^+$, **4′**, was detected by ESI-MS overnight.

Alkylation Reactions of 3. [Ru(bpy)$_2$(ttma-alcohol)](PF$_6$) was treated with excess acetic anhydride in refluxing CH_3CN. After 1 h, formation of [Ru(bpy)$_2$(ttma-acetate)]$^+$ was observed by ESI-MS as *m/z* 629. The reaction was left refluxing overnight, and [Ru(bpy)$_2$(ttma-acetate)]$^+$ was the most abundent peak in the spectra. In addition, traces of [Ru(bpy)$_2$(ttma-aldehyde)]$^+$, **4**, were seen as *m/z* 585.

A small amount (∼2 mg) of [Ru(bpy)$_2$(ttma-alcohol)](PF$_6$) was treated with excess MeI in methanol and stirred at room temperature under N_2. The reaction was monitored by ESI-MS, and after ∼24 h, an *m/z* 601 peak was oberserved, corresponding to the conversion of an alcohol to a methyl ether.

Acknowledgment. We thank Michael Goldfeld for his assistance with the EPR measurements and Prof. Andy Borovik for the use of his instrument. This research was supported by the American Cancer Society Research Scholar Grant (PJF RSG-03-251-01).

Supporting Information Available: ESI-MS analysis of oxidation and alkylation reactions, EPR spectra of bulk electrolysis, and further characterizations of complexes **1**–**4** including electronic spectra, IR absorbance spectra, ^{1}H NMR and 2D COSY NMR spectra, and crystal structures of complexes **1** and **2**.

IC7021962